Optik - International Journal for Light and Electron Optics 183 (2019) 131–136

Contents lists available at ScienceDirect

Optik

journal homepage: www.elsevier.com/locate/ijleo

Short note

Stable VCSEL mode discrimination realized by a ring-shaped dielectric relief☆

Yingying Liu[a,b], Youwen Huang[a,*], Xing Zhang[a,*], Jianwei Zhang[a], Yongqiang Ning[a], Lijun Wang[a]

[a] Changchun Institute of Optics, Fine Mechanics and Physics, Chinese Academy of Sciences, Changchun 130033, China
[b] University of Chinese Academy of Sciences, Beijing 100049, China

ARTICLE INFO

Keywords:
VCSEL
Higher-order modes
SiO_2 layer
Mode control

ABSTRACT

We demonstrated a method of transverse mode selection of vertical-cavity surface-emitting lasers (VCSELs). A ring-shaped anti-phase SiO_2 layer was introduced to filter the modes whose intensity distribution overlapped with the extra layer. The effective index method considering the size of the oxide aperture was applied to decide the inner/outer radius of the ring. Conventional reference device and two-round of confirmatory studies of ring-shaped SiO_2 VCSEL were fabricated and characterized. In comparison with the spectra of the conventional VCSEL, the VCSELs with ring-shaped SiO_2 layer emitted two stable transverse modes over the entire current range. This method may offer a new idea to solve the device request for the few-mode optical communications in the future.

1. Introduction

Vertical cavity surface emitting lasers (VCSELs) have numerous unique advantages, such as single longitudinal mode output, circular beam, ease of two-dimensional array formation and high modulation bandwidth, making VCSELs a key component for optical communications [1,2].

To cater to the requirements of increasingly information driven society and economy, the higher-capacity and faster-speed fiber-optic communication and optical interconnects systems are extensively demanded. The capacity increase and between the continuing growth of mobile internet application and services is supplement and promote each other, and both of them drive next generation wireless communication network. However, we are facing difficulty of near peak transmission-capacity of air-interface spectrum efficiency. In terms of carrier wave, the exploitable freedoms of frequency, polarization, amplitude and phase have been exhausted in wave division multiplexing (WDM) technology [3]. Therefore, the wireless communications system capacity increase in the next decade would be driven by the upgrades in devices, network architecture improvements as well as information and communication technology convergence. Space-division multiplexing (SDM) including core multiplexing and mode-division multiplexing (MDM) over few-mode fiber (FMF) is likely to become a promising technology to overcome the capacity crunch [4–7]. Already some densely packed VCSEL arrays have been fabricated for high-speed communication [8,9]. In MDM technologies, the optical signals from VCSEL

☆ Supported by the National Key Research and Development Program (2016YFE0126800); National Natural Science Foundation of China (61434005, 11774343, 11674314, and 61727822); the Science and Technology Program of Jilin Province, China (20180201119GX) and the Youth Innovation Promotion Association of China (2017260).

* Corresponding authors.
E-mail addresses: huangyouwen13@mails.ucas.ac.cn (Y. Huang), zhangx@ciomp.ac.cn (X. Zhang).

https://doi.org/10.1016/j.ijleo.2019.02.098
Received 12 January 2019; Accepted 20 February 2019

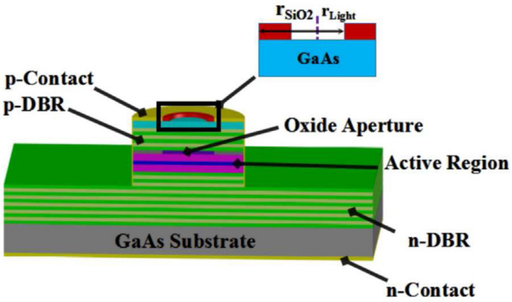

Fig. 1. The cross sectional view of ring-shaped SiO_2 VCSEL: here r_{sio2} represents the outer radius of SiO_2 ring; r_{light} represents the inner radius of SiO_2 ring.

arrays should be combined into a bundle of single-mode fibers with different modes or separate cores by multiplexers (MUXs) [10]. Whereas some VCSEL arrays are not compact enough for coupling into FMFs without sophisticated coupling optics [11–15]. Therefore, developing a single VCSEL with controllable numbers of transverse modes simultaneously and carrying more information is meaningful. The immature few-mode vertical cavity surface emitting laser (VCSEL) has been employed to explore new technology to increase transmission capacity. However, there is no confirmative effective method to develop few-mode VCSEL until now.

In this paper, we proposed a stable two transverse mode emitting VCSEL with a SiO_2 ring-shaped mode filter layer. This method avoids redesign of epitaxial structure and precise etching depth control of surface relief. We can obtain same functions as the conventional surface relief by adjusting thickness of the current insulation layer and the inner/outer radius. The dielectric film was deposited on the surface of VCSEL through the PECVD. The current injection window and the ring-shaped mode filer were simultaneously formed by a single exposure and etching process. The size of the oxide aperture and the ring-shaped dielectric layer was decided by the simulation results of effective index model. A conventional reference device and a VCSEL with ring-shaped mode filter layer were fabricated and characterized.

2. Device structure

Many efforts have been implemented to control the numbers of transverse modes of large oxide aperture VCSELs: photonic crystal waveguides [16], wedge-shaped holey structures [17], micro-lens [18], Zn diffusion structure [19] and etched surface relief [20–22]. Here we take advantages of a non-destructive relief method allows for mode selection by depositing a dielectric anti-phase ring-shape SiO_2 layer. The epitaxial structure of the 850 nm VCSEL was shown in Fig. 1. The VCSEL consisted of a Si-doped distribute Bragg reflector (DBR) stacked up with 34 pairs of $Al_{0.12}Ga_{0.88}As/Al_{0.9}Ga_{0.1}As$ layers. Three 7.2 nm thick GaAs strained quantum wells were embedded in the center of one-wavelength thick $Al_{0.3}Ga_{0.7}As$ spacer. A 30-nm-thick $Al_{0.98}Ga_{0.02}As$ layer was inserted on top of the p-spacer layer and oxidized to form the current and light confinement aperture with diameter of 6 μm. The p-DBR contained 20.5 pairs of C-doped $Al_{0.12}Ga_{0.88}As$/ $Al_{0.9}Ga_{0.1}As$. A heavily doped p-GaAs contact layer was deposited to increase the efficiency of current injection. The SiO_2 membrane was deposited by plasma enhanced chemical vapor deposition (PECVD) technology on top-surface of VCSEL. The ring-shaped SiO_2, current injection window and the out window of the light were obtained simultaneously through a single self-aligned photoresist process.

3. Simulation

An effective index model was modeled to investigate the influence of oxide size on the transverse modes characteristics in large oxide aperture VCSELs and to determine the size of the ring-shaped [23]. The relationship between mode-order supported by the oxide confined VCSEL and the size of the oxide aperture was shown in Fig. 2. We can see that the fundamental mode (LP_{01}) can be obtained when the diameter of oxide aperture was less than 3 μm. The VCSEL supported much more transverse mode and shown a non-linear growth with the enlarging of the diameter of oxide aperture. Therefore, few-mode can be emitted from the unprocessed VCSEL when diameter of oxide aperture was kept 4–6 μm. In this work, the diameter of oxide aperture was determined to be 6 μm, 8 modal orders could be excited from the VCSELs in normal work condition accordingly. The ring-shaped SiO_2 relief was introduced into conventional VCSEL to filter extra transverse mode. The ring with outer radius of 4 μm and the inner radius of 1.7 μm was confirmed by considering to introduce a $\pi/2$ phase jump in the areas of SiO_2 covering. The region from the outer radius of the ring to the mesa edge was covered by p-metal.

The transfer matrix method was applied to calculate the reflectivity of the p-side of the VCSEL with different thickness of SiO_2 layer. In the calculation, the SiO_2 layer were divided into large numbers of slices, and the numbers of the matrix element of slice was related to the variation in SiO_2 thickness. Simultaneously, we also calculated the mirror loss effected by the extra SiO_2 layer. The calculation results were shown in Fig. 3. A maximum mirror-loss and a minimum reflectivity can be obtained when the SiO_2 layer reached a thickness of 145 nm, respectively. That was caused by a $\pi/2$ phase jump introduced by a quarter of the optical thickness SiO_2 layer. Thus, the regions covered with the SiO_2 layer suffered from a larger mirror-loss and threshold gain, and the modes emitted from these areas can be suppressed. The mesa center of VCSEL, encircled by the ring-shaped SiO_2, suffered less mirror-loss. The

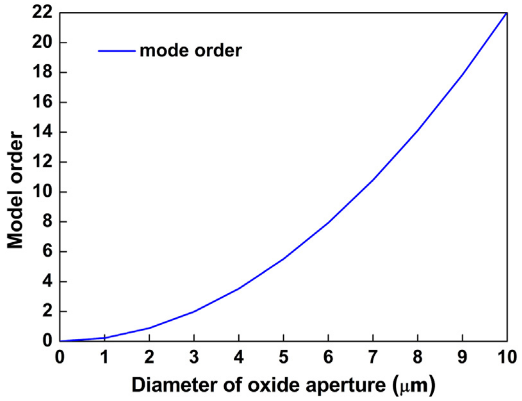

Fig. 2. The simulation of 6 μm oxide-confined VCSEL: the transverse mode order probably excites with respect to oxide aperture.

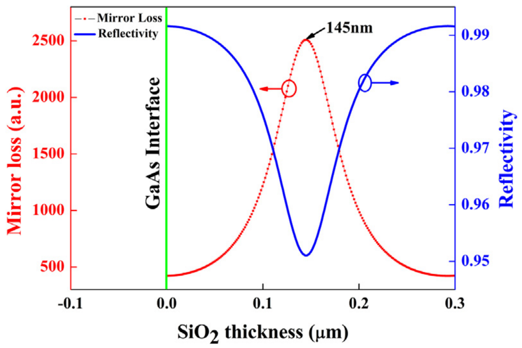

Fig. 3. The simulation of 6 μm oxide-confined VCSEL: (red) the relationship between mirror loss and SiO_2 thickness; (blue) the relationship between reflectivity and SiO_2 thickness.

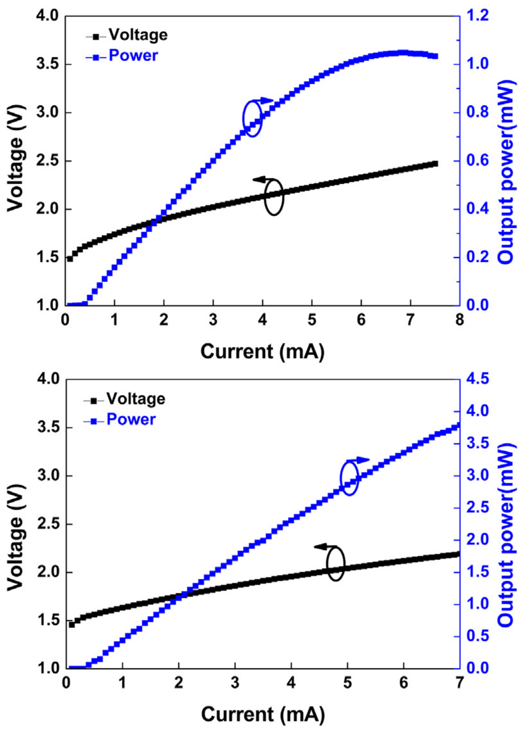

Fig. 4. The *P–I–V* characteristics in comparison between (a) the ring-shaped SiO_2 and (b) conventional VCSELs at room temperature.

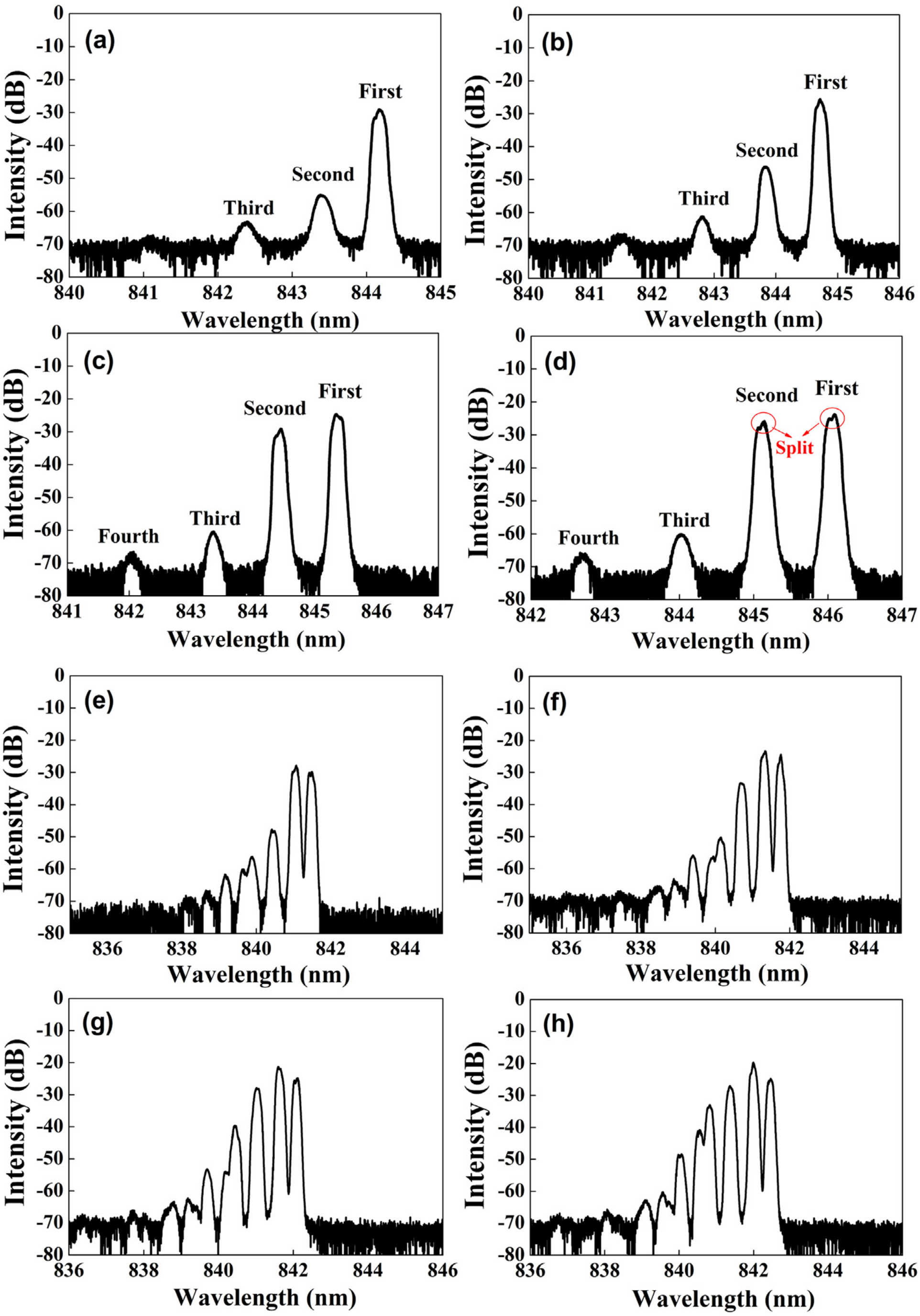

Fig. 5. (a–d) Spectra of the ring-shaped SiO_2 VCSEL at various currents: (a) $I = 1$ mA; (b) $I = 2$ mA; (c) $I = 3$ mA; (d) $I = 4$ mA; (e–h) Spectra of the conventional VCSEL at various currents: (e) $I = 1$ mA; (f) $I = 24$ mA; (g) $I = 3$ mA; (h) $I = 4$ mA.

modes emitted from center had a much smaller threshold gain to be lased in priority.

4. Results and discussion

The power–current–voltage (*P*–*I*–*V*) characteristics of the VCSEL with a ring-shaped SiO_2 layer and conventional VCSEL were measured under the continuous-wave (CW) condition at room temperature and shown in Fig. 4. The VCSEL with a ring-shaped SiO_2 has a turn-on voltage of 1.487 V, a threshold current of 0.5 mA and a maximum output power of 1.048 mW. The conventional VCSEL shows a turn-on voltage of 1.456 V and a threshold current of 0.6 mA. Compared with the conventional VCSEL, the slope of the *I*–*V*

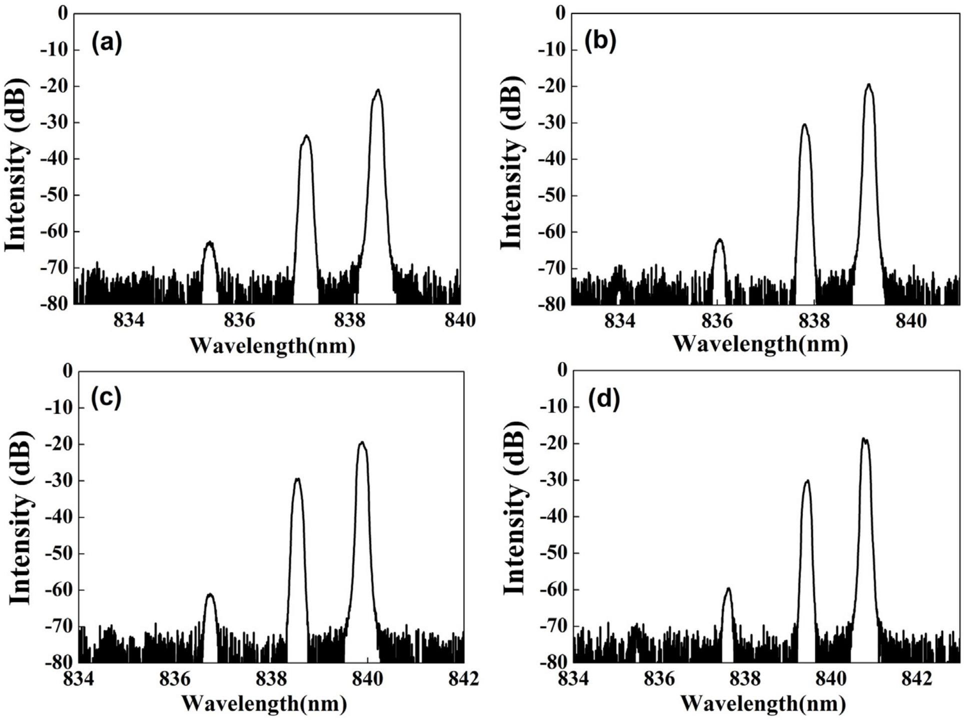

Fig. 6. (a–d) spectra of the ring-shaped SiO_2 VCSEL at various current: (a) I = 1 mA; (b) I = 2 mA; (c) I = 3 mA; (d) I = 4 mA.

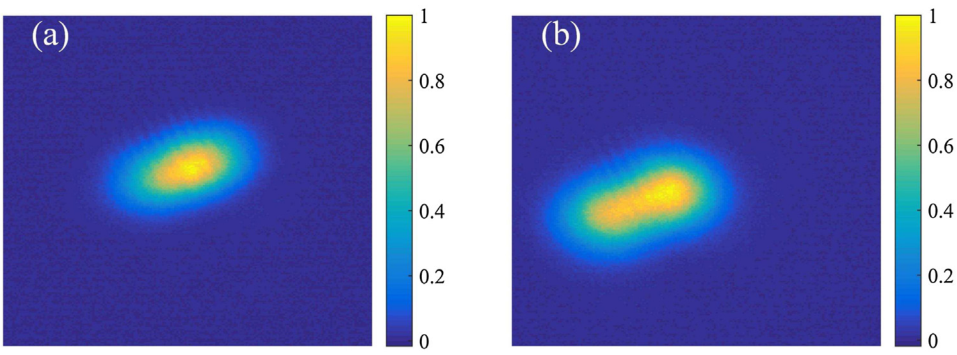

Fig. 7. Near-field pattern of the ring-shaped SiO_2 VCSEL. (a) I = 1 mA; (b) I = 5 mA.

curve of the ring-shaped SiO_2 VCSEL is larger, indicating a slightly higher series resistance. The VCSEL with ring-shaped SiO_2 is lower in output power than the conventional VCSEL. The ring-shaped SiO_2 acts as a dielectric phase structure and control the number of emitting modes. The higher-order modes suffer a significant loss and are suppressed naturally. The suppression of higher-order modes leads to the decrease of total output power compared with the conventional VCSEL. An earlier thermal roll-over occurs under the same measurement condition. That can be explained by the power of those suppressed modes were transferred to self-heating, thus decreasing the device efficiency.

A stable two modes lasing property were achieved on the device of VCSEL with a ring-shaped SiO_2 layer. The spectra of the ring-shaped SiO_2 VCSEL and conventional VCSEL were tested and shown in Fig. 5(a–d) and (e–h), respectively. Fig. 5(a–d) shows spectra of the ring-shaped SiO_2 VCSEL at current of 1 mA, 2 mA, 3 mA and 4 mA. It can be seen that the first two modes were stable emitted along with the increase of current. The spectra intensity of them is higher than the third and fourth modes with more than 25 dB at 3 mA and 4 mA. The first fundamental mode (LP_{01}) and second higher-order mode (LP_{11}) are naturally orthogonal, and the split between them is approximately 1 nm. Fig. 5(e–h) shows the spectra of conventional VCSEL at 1 mA, 2 mA, 3 mA and 4 mA. Large numbers of modes can be observed simultaneously due to the large oxide aperture size of 6 μm.

To verify the reliability and repeatability of the dielectric phase structure design, another wafer was used to repeat all of the fabrication process of the previous VCSEL with a ring-shaped SiO_2. Since we were only concerned about the transverse mode effected by the ring-shaped SiO_2 layer, the high-resolution spectra (resolution = 0.02 nm, 0.02 nm is narrow enough to distinguish the transverse mode of the VCSEL) were measured at 1 mA, 2 mA, 3 mA and 4 mA, and they were shown in Fig. 6(a)–(d), respectively.

Similarly, only two dominated modes appeared at different currents. That is in agreement with the measured results presented in Fig. 5(a–d). The introduced ring-shaped SiO_2 serves as a mode discriminator for the conventional VCSEL. The spectra prove that the ring-shaped SiO_2 provides mode selectivity to suppress higher order modes.

Additionally, the near-field patterns of the VCSEL with a ring-shaped SiO_2 at 1 mA and 5 mA were measured and shown in Fig. 7. Only the lobe of first fundamental mode was detected in Fig. 7(a) when the current was at 1 mA, which coincided with the result of spectrum in Fig. 5(a). Two lobes were close enough and unable to be distinguished in Fig. 7(b) when the current increased to 5 mA, the near-field pattern always remained stable two lobes.

5. Conclusion

In summary, it is demonstrated a stable two transverse mode VCSEL with 6 μm oxide aperture were achieved by use of the ring-shaped SiO_2 dielectric anti-phase filter. Base the simulation, the inner and outer radius of ring-shaped SiO_2 was defined with 1.7 μm and 4 μm, and the thickness was set by 145 nm. Conventional reference device and two-round of confirmatory studies of ring-shaped SiO_2 VCSEL were fabricated and characterized. Both of the spectra and near-field measurement of ring-shaped SiO_2 VCSEL displayed the stable two modes emitting under different current. This mode discrimination method improves the modal properties of the VCSEL without extra fabrication step compared to the conventional VCSEL and has a great potential application in few-mode VCSEL and the corresponding few-mode optical communication.

References

[1] K. Iga, Surface-emitting laser – its birth and generation of new optoelectronics field, IEEE J. Sel. Top. Quantum Electron. 6 (6) (2000) 1201–1215, https://doi.org/10.1109/2944.902168.

[2] D.M. Kuchta, A.V. Rylyakov, F.E. Doany, C.L. Schow, J.E. Proesel, C.W. Baks, P. Westbergh, J.S. Gustavsson, A. Larsson, A 71 Gb/s NRZ modulated 850 nm VCSEL-based optical link, IEEE Photon. Technol. Lett. 27 (6) (2015) 577–580, https://doi.org/10.1109/LPT.2014.2385671.

[3] R.-J. Essiambre, G. Kramer, P.J. Winzer, G.J. Foschini, B. Goebel, Capacity limits of optical fiber networks, J. Lightwave Technol. 28 (4) (2010) 662–701, https://doi.org/10.1109/JLT.2009.2039464.

[4] D.J. Richardson, J.M. Fini, L.E. Nelson, Space-division multiplexing in optical fibres, Nat. Photonics (2013) 1–9, https://doi.org/10.1038/nphoton.2013.94.

[5] E. Ip, N. Bai, Y.K. Huang, E. Mateo, F. Yaman, M.J. Li, S. Bickham, S. Ten, J. Liñares, C. Montero, V. Moreno, X. Prieto, V. Tse, K.M. Chung, A. Lau, H.Y. Tam, C. Lu, Y. Luo, G.D. Peng, G. Li, 88 × 3 × 112-Gb/s WDM transmission over 50 km of three-mode fiber with inline few mode fiber amplifier, ECOC, OSA, Washington, D.C. (2011), https://doi.org/10.1364/ECOC.2011.Th.13.C.2 p. Th.13.C.2.

[6] S. Randel, R. Ryf, A. Sierra, P.J. Winzer, A.H. Gnauck, C.A. Bolle, R.-J. Essiambre, D.W. Peckham, A. McCurdy, R. Lingle, 6 × 56-Gb/s mode-division multiplexed transmission over 33-km few-mode fiber enabled by 6 × 6 MIMO equalization, Opt. Express 19 (17) (2011) 16697–16707, https://doi.org/10.1364/OE.19.016697.

[7] A. Al Amin, A. Li, S. Chen, X. Chen, G. Gao, W. Shieh, Dual-LP_{11} mode 4 × 4 MIMO-OFDM transmission over a two-mode fiber, Opt. Express 19 (17) (2011) 16672–16679, https://doi.org/10.1364/OE.19.016672.

[8] A. Larsson, P. Westbergh, J.S. Gustavsson, E. Haglund, E.P. Haglund, High-speed VCSELs and VCSEL arrays for single- and multi-core fiber interconnects, SPIE OPTO, SPIE, 2015, pp. 93810D–12, , https://doi.org/10.1117/12.2082614.

[9] C. Xie, S. Spiga, P. Dong, P. Winzer, M. Bergmann, B. Kogel, C. Neumeyr, M.-C. Amann, 400 Gb/s PDM-4PAM WDM system using a monolithic 2 × 4 VCSEL array and coherent detection, J. Lightwave Technol. 33 (3) (2015) 670–677, https://doi.org/10.1109/JLT.2014.2363017.

[10] H. Chen, A.M.J.T. Koonen, Spatial division multiplexing, in: H. Venghaus, N. Grote (Eds.), Fibre Optic Communication: Key Devices, Springer Series in Optical Sciences, Cham, 2017, pp. 1–48, , https://doi.org/10.1007/978-3-319-42367-8_1.

[11] S.Y. Hu, J. Ko, E.R. Hegblom, L.A. Coldren, Multimode WDM optical data links with monolithically integrated multiple-channel VCSEL and photodetector arrays, IEEE J. Quantum Electron. 34 (8) (1998) 1403–1414, https://doi.org/10.1109/3.704330.

[12] Y.-G. Ju, D. Lofgreen, A. Fiore, S.-Y. Hu, E. Hegblom, D. Louderback, O. Sjolund, A. Huntington, L.A. Coldren, Densely packed pie shaped vertical-cavity surface-emitting laser array incorporating a tapered one-dimensional wet oxidation, IEEE Photon. Technol. Lett. 12 (5) (2000) 462–464, https://doi.org/10.1109/68.841253.

[13] M.T. Johnson, D.F. Siriani, M. Peun Tan, K.D. Choquette, Beam steering via resonance detuning in coherently coupled vertical cavity laser arrays, Appl. Phys. Lett. 103 (20) (2013) 201115, https://doi.org/10.1063/1.4830432.

[14] H. Roscher, P. Gerlach, F.N. Khan, A. Kroner, M. Stach, A. Weigl, R. Michalzik, Toward more efficient fabrication of high-density 2-D VCSEL arrays for spatial redundancy and/or multi-level signal communication, Photonics Europe, SPIE, 2006, p. 61850V, , https://doi.org/10.1117/12.662121.

[15] H. Roscher, F. Rinaldi, R. Michalzik, Small-pitch flip-chip-bonded VCSEL arrays enabling transmitter redundancy and monitoring in 2-D 10-Gbit/s space-parallel fiber transmission, IEEE J. Sel. Topics Quantum Electron. 13 (5) (2007) 1279–1289, https://doi.org/10.1109/JSTQE.2007.905150.

[16] A.J. Danner, T.S. Kim, K.D. Choquette, Single fundamental mode photonic crystal vertical cavity laser with improved output power, Electron. Lett. 41 (6) (2005) 325, https://doi.org/10.1049/el:20057841.

[17] A. Furukawa, S. Sasaki, M. Hoshi, A. Matsuzono, K. Moritoh, T. Baba, High-power single-mode vertical-cavity surface-emitting lasers with triangular holey structure, Appl. Phys. Lett. 85 (22) (2004) 5161–5163, https://doi.org/10.1063/1.1830071.

[18] Y. Huang, X. Zhang, J. Zhang, Y. Xie, W. Hofmann, Y. Ning, L. Wang, Monolithic microlens VCSELs with high beam quality, IEEE Photonics J. 9 (4) (2017) 1–8, https://doi.org/10.1109/JPHOT.2017.2719702.

[19] E.W. Young, K.D. Choquette, S.L. Chuang, K.M. Geib, A.J. Fischer, A.A. Allerman, Single-transverse-mode vertical-cavity lasers under continuous and pulsed operation, IEEE Photon. Technol. Lett. 13 (9) (2001) 927–929, https://doi.org/10.1109/68.942649.

[20] H. Martinsson, J.A. Vukusic, M. Grabberr, R. Michalzik, R. Jager, K.J. Ebeling, A. Larsson, Transverse mode selection in large-area oxide-confined vertical-cavity surface-emitting lasers using a shallow surface relief, IEEE Photon. Technol. Lett. 11 (12) (1999) 1536–1538, https://doi.org/10.1109/68.806837.

[21] A. Haglund, J.S. Gustavsson, J. Vukusic, P. Modh, A. Larsson, Single fundamental-mode output power exceeding 6 mW from VCSELs with a shallow surface relief, IEEE Photon. Technol. Lett. 16 (2) (2004) 368–370, https://doi.org/10.1109/LPT.2003.821085.

[22] A. Kroner, F. Rinaldi, J.M. Ostermann, R. Michalzik, High-performance single fundamental mode AlGaAs VCSELs with mode-selective mirror reflectivities, Opt. Commun. 270 (2) (2007) 332–335, https://doi.org/10.1016/j.optcom.2006.09.011.

[23] A. Valle, J. Sarma, K.A. Shore, Spatial hole-burning effects on the dynamics of vertical cavity surface-emitting laser diodes, IEEE J. Quantum Electron. 31 (8) (1995) 1423–1431, https://doi.org/10.1109/3.400393.